

CARDIOVASCULAR IMAGING IN CLINICAL AND EXPERIMENTAL ACUTE INFECTIOUS MYOCARDITIS

Jamshid Shirani^{1,3}, Arzu Ilercil¹, Madhulika Chandra¹, Linda A. Jelicks⁴, Herbert B. Tanowitz^{2,4}

¹ Department of Medicine, Division of Cardiology and ² Infectious Diseases, ³ Department of Pathology, and ⁴ Department of Physiology and Biophysics, Albert Einstein College of Medicine, Bronx, New York

TABLE OF CONTENTS

1. Abstract
2. Introduction
3. Cardiac imaging in clinical myocarditis
 - 3.1. Echocardiography
 - 3.2. Magnetic resonance imaging
 - 3.3. Nuclear imaging
4. Chagasic myocarditis and cardiomyopathy
5. Bacterial myocarditis
6. Acquired immunodeficiency syndrome
7. Peripartum cardiomyopathy
8. Cardiac imaging in experimental models of myocarditis
 - 8.1. Echocardiography
 - 8.1.1. *Trypanosoma cruzi* infection
 - 8.1.2. Future directions
 - 8.2. Magnetic resonance imaging
 - 8.2.1. *Trypanosoma cruzi* infection
 - 8.2.2. Tumor necrosis factor
 - 8.2.3. Future directions
9. Conclusions
10. Acknowledgements
11. References

1. ABSTRACT

Acute myocarditis can be caused by a variety of organisms. Congestive heart failure and death may occur as a consequence of these infections. In recent years cardiac imaging, by echocardiography and magnetic resonance and nuclear imaging has become a useful adjunct in the diagnosis and management of infectious myocarditis. Specific examples of their usefulness will be given in the discussions of chagasic myocarditis, bacterial myocarditis, acquired immunodeficiency syndrome and peripartum cardiomyopathy. Finally, we explore the exciting area of cardiac imaging of small animals, such as mice infected with *Trypanosoma cruzi*.

2. INTRODUCTION

Acute myocarditis is an important cause of sudden death and congestive heart failure in children and young adults. Over the last decade, significant advances have been made in diagnosis and management of acute myocarditis, greatly assisted by the development of imaging techniques used in the clinical disease. Thus, echocardiography, magnetic resonance imaging, and nuclear scintigraphic imaging techniques have been used successfully to assess cardiovascular function during acute infection, obtain valuable prognostic information, determine the course of the disease, and evaluate the cardiovascular complications of clinical acute myocarditis.

In addition, new imaging techniques, such as tissue characterization by ultrasound or magnetic resonance imaging may soon provide complementary information to that obtained by histologic evaluation of myocardial samples obtained by endomyocardial biopsy. Other techniques such as tissue Doppler or strain rate echocardiography have not been systematically used in evaluation of patients with acute myocarditis and have the potential to offer means of monitoring progression of the disease and its response to treatment.

Serial noninvasive cardiac evaluation, particularly with the use of echocardiography or magnetic resonance imaging, has been instrumental in understanding the pathophysiologic mechanisms involved in acute myocarditis when applied to a multitude of experimental models of the disease. These imaging techniques have been used to assess the time course and progression of cardiac abnormalities in intact animals as well as determine the significance of the genetic background, age, gender, and immunologic status of the host in response to myocardial infection.

The aim of this report is to provide a brief overview of the use of noninvasive cardiac imaging techniques in the assessment of clinical and experimental acute myocarditis.

Table 1. Infectious Etiologies of Human Acute Myocarditis

Viruses	<ul style="list-style-type: none"> • Coxsackievirus (A and B), Echovirus, Cytomegalovirus, Adenovirus • Human immunodeficiency virus-1 • Less common agents: Poliovirus, Influenza virus, Hepatitis (B or C), Encephalomyocarditis virus, Respiratory syncytial virus, Rabies, Rubella, Rubeola, Vaccinia, Varicella, Variola, Yellow fever
Chlamydia/Atypical agents	<i>Mycoplasma pneumoniae</i> , Psittacosis
Bacteria	Streptococcus, Staphylococcus, Pneumococcus, Meningococcus, <i>Hemophilus</i> , Gonococcus, Brucellosis, Diphtheria, Salmonellosis, Tuberculosis, Tularemia, Actinomycosis
Spirochetes	Leptospirosis, Lyme disease, Relapsing fever, Syphilis
Fungi	Aspergillosis, Actinomycosis, Blastomycosis, Candidiasis, Coccidioidomycosis, Cryptococcosis, Histoplasmosis, <i>Pneumocystis</i>
Protozoa	<i>Trypanosoma cruzi</i> , <i>Toxoplasma gondii</i> , Malaria, Amebiasis, microsporidiosis
Metazoa	Trichinosis, Schistosomiasis, Ascariasis, Echinococcosis, Cysticercosis

3. CARDIAC IMAGING IN CLINICAL MYOCARDITIS

3.1. Echocardiography

Echocardiography is frequently used to evaluate patients with suspected acute infectious myocarditis. Its utility is not only to aid in the diagnosis but also to identify complications and to provide prognostic information. Despite the critical role of echocardiography in the evaluation of infectious myocarditis, there is a paucity of published reports regarding its use. This may reflect the sporadic and indolent nature of many infectious causes of myocarditis (Table 1), the existence of only a few centers that evaluate adequate number of such patients, and the inherent difficulties in establishing an infectious etiology, especially when presentation is late in the course of the disease. In this section, we review the current literature dealing specifically with the use of echocardiography in clinical infectious myocarditis. The general echocardiographic features of the disease, its complications, and prognostic findings are reviewed. Echocardiographic features of several specific etiologies of acute myocarditis are reviewed in subsequent sections.

Echocardiographic features of acute infectious myocarditis are variable and often differ depending on the causative agent and on the timing of evaluation in relation to the disease onset. Early in the course of the disease, echocardiography may show minimal structural cardiac abnormalities as myocyte necrosis and inflammation commonly begins in the epicardial region (Figure 1). As myocarditis progresses towards the endocardium, reversible or irreversible, diffuse or regional left and/or right ventricular dysfunction are often seen on echocardiography. Later during the disease, features of dilated cardiomyopathy are seen, characterized by enlarged cardiac chambers and impaired systolic and diastolic function of the left and right ventricles (Figure 2).

In an early report, a consecutive series of 68 patients diagnosed with acute infectious myocarditis based on clinical presentation, were evaluated by M-mode echocardiography to identify the relationship between alterations of cardiac function and clinical severity of myocarditis (1). Patients were classified as having mild myocarditis when only electrocardiographic abnormalities

were present, moderate myocarditis when clinical findings consistent with left ventricular dysfunction were present and severe myocarditis when presentation was associated with clinically severe congestive heart failure. In this series, marked left ventricular and left atrial chamber dilation and significant reduction in left ventricular shortening fraction and ejection fraction was seen only in patients with severe myocarditis. However, localized left ventricular wall motion abnormalities were reported in all patients and the extent of regional dysfunction (number of asynergic segments) correlated with the severity of the clinical presentation. In the absence of diffuse left ventricular dysfunction, regional asynergy more frequently involved the inferior (18/68 (26%)) and anterior (12/68(18%)) myocardial regions and less often the posterolateral region (6/68 (9%)). Patients with mild myocarditis were commonly found to have hyperkinesis of uninvolved left ventricular regions (37/40 (92%)), a finding less frequently present in those with moderate myocarditis (14/21 (67%) patients) and not found in patients with severe myocarditis. Pericardial effusion was found in 10% of patients in this report and did not correlate with the severity of the clinical presentation.

In another series, 41 patients with histologically established myocarditis were evaluated by M-mode and two-dimensional echocardiography (2). In this report, 50% of patients had increased left ventricular end-diastolic diameter and reduced systolic function as assessed by fractional shortening, 1 patient had a dilated left ventricle with preserved systolic function and 14 (36%) patients had normal left ventricular size and systolic function. Segmental wall motion abnormalities were observed in 25 (64%) patients and included regional hypokinesis, akinesis, dyskinesis, or aneurysm. Increased right ventricular end-diastolic area was observed in 8 (20%) patients of whom 3 had reduced systolic function. In another 5 patients, right ventricular systolic function was diminished despite normal chamber sizes. Mild increases in left ventricular wall thickness (>11mm) was seen in 6 patients and was diffuse in 2 and localized to the papillary muscles in the remaining 4 patients. In 2 patients presenting initially with normal left ventricular wall thickness, follow-up echocardiographic evaluations at the time of clinical improvement demonstrated transiently increased wall thickness that

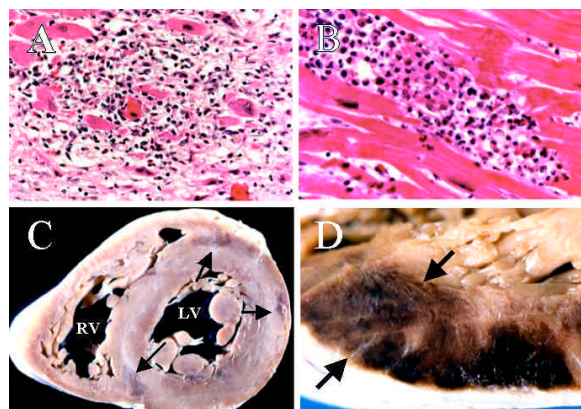


Figure 1. Transverse section of the heart at mid-ventricular level (C) showing predominantly epicardial lesions (arrows). More extensive, transmural involvement is shown in close-up view of the left ventricular myocardium (D). The lesions spare the endocardial most portion of the myocardium (D, arrows). Histologic sections (stained with hematoxylin & eosin) show mononuclear cellular infiltration and myocyte necrosis (A and B).

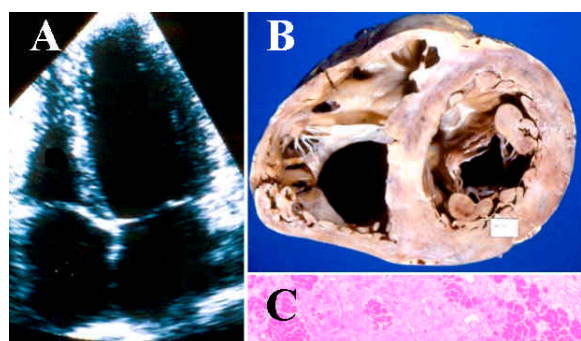


Figure 2. Two-dimensional echocardiographic image of the heart of a patient with end-stage cardiomyopathy late after acute myocarditis (A). Cardiac chambers are dilated. Patchy areas of myocardial fibrosis are seen on the gross (B) and histologic (C) sections (hematoxylin & eosin) of the heart.

resolved in the subsequent months. Ventricular thrombi were not infrequent in this series (15 % of patients) and were most often detected in the left ventricle, but were also found in both ventricles simultaneously or in the right ventricle alone in some patients. Altered myocardial texture characterized by generally small areas of increased reflectivity, were observed in 9 patients (23%). These areas were most often localized to the ventricular septum or the papillary muscles. Additional findings noted in this report included abnormalities of left ventricular diastolic filling ($n=8$ (20%)) that were visually characterized as an initial rapid filling with subsequent abrupt cessation ("restrictive physiology"). In 3 of these patients, a restrictive pattern of left ventricular diastolic filling (dip and plateau pattern on pressure tracings) was demonstrated by catheterization.

In a more recent report (3), echocardiographic findings at baseline and at 6 months following the

presentation were evaluated in two groups of patients with either fulminant ($n=11$) or acute ($n=43$) myocarditis. Fulminant myocarditis was defined as sudden onset of severe hemodynamic compromise and marked myocardial inflammation as opposed to the less severe hemodynamic abnormality, indistinct onset of symptoms and more variable degree of myocardial inflammation in those with acute myocarditis. Both groups of patients were noted to have severely depressed left ventricular systolic function of similar magnitude at baseline. However, those with fulminant myocarditis had less significant left ventricular dilation (end-diastolic diameters 5.3 ± 0.9 -vs- 6.1 ± 0.8 cm) and greater septal wall thickness (1.2 ± 0.2 -vs- 1.0 ± 0.8 cm). At the 6-month follow-up, significant improvement in left ventricular systolic function was noted in patients with fulminant and not in those with acute myocarditis. Left ventricular diastolic diameter did not significantly change over time in the two groups, although there was a trend towards a reduction in left ventricular septal thickness in those with fulminant myocarditis. Other investigators have also reported transient increases in left ventricular wall thickness during acute infectious myocarditis (4). This may affect the left ventricular wall in a homogeneous or a regional manner and is thought to represent myocardial edema in areas of intense inflammation. It is also shown that failure of improvement in left ventricular ejection fraction in the first 6 months following presentation is associated with a high likelihood (59%) of death (5). Thus, certain echocardiographic findings on presentation, and serial evaluation during convalescence, may provide useful prognostic markers in patients with myocarditis.

The echocardiographic findings in infectious myocarditis may be nonspecific and at times may mimic other causes of left ventricular dysfunction including idiopathic dilated cardiomyopathy, non-infectious myocarditis or ischemic heart disease. In fact, in some patients with acute infectious myocarditis, the echocardiographic, clinical and electrocardiographic findings are indistinguishable from those of acute myocardial infarction (6). In addition, left ventricular wall motion abnormalities found on echocardiography in patients with acute myocarditis can be transient and may resolve rapidly or within several months (1,6,7). The findings emphasize the fact that the echocardiographic abnormalities suggestive of acute myocarditis must be interpreted in the context of the entire clinical presentation. Transient left ventricular apical dyskinesia with associated apical thrombus formation and subsequent systemic embolization has been reported in acute myocarditis (8). As mentioned above, left ventricular apical thrombus may be present in as many as 15% of patients with acute myocarditis studied by echocardiography (2).

Newer echocardiographic techniques including ultrasonic tissue characterization and Doppler measures of diastolic function are being increasingly used in the evaluation of myocarditis (9) and may provide further diagnostic and prognostic parameters. Ultrasonic tissue characterization relates the intensity of the backscattered myocardial signal to tissue composition especially the collagen content. Thus, patients with persistent or healed

Imaging in myocarditis

myocarditis demonstrate an increased intensity of the backscattered myocardial ultrasonic signal compared with normal individuals (10). However, in its present form, this technique is unable to differentiate myocarditis from other causes of myocardial edema or fibrosis.

3.2. Magnetic resonance imaging

Experience with magnetic resonance imaging in acute myocarditis is limited. However, this technique has the potential to aid in the diagnosis of acute myocarditis. Early in the course of the disease, the myocardium produces high signal intensity on the T2-weighted sequences by magnetic resonance imaging due to the presence of edema (11). In a preliminary study, myocardial edema was identified by magnetic resonance imaging in regions of hypokinesis or akinesis (on echocardiography) in 2 patients with acute myocarditis (12). This finding resolved on repeat magnetic resonance imaging after recovery of left ventricular function in both patients. In another study of 11 children with suspected myocarditis, tissue characterization by magnetic resonance imaging in the myocardial region of interest was predictive of histologic findings of myocarditis (13). It is also suggested that acute myocarditis may be associated with an initially focal, followed by a global, increased myocardial signal enhancement following injection of contrast (gadolinium) during gated magnetic resonance imaging (14).

3.3. Nuclear imaging

Gallium-67 cardiac scintigraphic imaging has been used as a screening tool to identify patients with inflammatory myocardial disease (15). O'Connell et al (16) examined the applicability of gallium-67 myocardial imaging in 68 patients with dilated cardiomyopathy. Only 1 of 57 patients with a negative gallium-67 scan showed evidence of myocarditis by endomyocardial biopsy (negative predictive value 98%). On the other hand, only 5 of 14 patients with a positive gallium-67 scan showed biopsy evidence of acute myocarditis (positive predictive value 36%). Authors noted that mediastinal uptake of the tracer may obscure cardiac uptake and lead to a false negative study in an occasional patient. Follow up scans in patients with biopsy-proven myocarditis closely related to the findings at histology. It was concluded that gallium-67 myocardial scintigraphic imaging is a useful screening tool for myocarditis and may obviate the need for repeat endomyocardial biopsies in the assessment of the response to therapy in those with histologic evidence of the disease. Because substantial expertise is required for proper acquisition and interpretation of these scans, few centers continue to perform gallium-67 myocardial scans in large enough numbers. The introduction of single photon emission computed tomography has improved the differentiation of myocardial from pericardial uptake of gallium-67 compared with planar images alone (17). It should be noted that gallium-67 acts as a ferric ion analog and is bound to transferrin, lactoferrin and other plasma proteins. The exact reason for the accumulation of the tracer at sites of infection and inflammation is not well understood and is likely complex.

Indium-111 antimyosin antibodies bind specifically to exposed heavy chain myosin in damaged myocardial cells, thereby allowing noninvasive diagnosis

of myocardial necrosis (18) and providing a means to monitor ongoing necrotic cell loss in myocarditis (19). Typical anti-myosin antibody scan shows a diffuse, faint and heterogeneous uptake in acute myocarditis, as opposed to the intense, localized uptake of the antibody in acute myocardial infarction. A normal anti-myosin antibody scan essentially excludes acute myocarditis and acute myocardial infarction (18). The negative predictive value of indium-labeled antimyosin antibody scanning probably exceeds that of gallium-67 imaging, although it has varied based on the gold standard used for comparison. Dec et al (20) demonstrated a sensitivity of 83%, specificity of 53%, and a negative predictive value of 92% for anti-myosin antibody scanning, compared with endomyocardial biopsy, in a series of 82 patients. The presence of a positive scan on presentation was also highly predictive of improvement in left ventricular systolic function within 6 months in this group of patients. It is predicted that when this type of myocardial imaging becomes commercially available, it would provide a sensitive screening tool for exclusion of myocardial necrosis. The specificity of this test, however, will remain low because the high affinity of the tracer for necrotic myocytes would lead to a positive scan in any condition associated with myocardial necrosis (21-24).

More widely available nuclear imaging techniques, such as radionuclide ventricular angiography using technetium-99 tagged red blood cells, have also been used for the evaluation of patients with acute myocarditis. Quigley et al (25) studied 23 patients with biopsy-proven acute myocarditis at baseline and 6-8 months after their initial presentation. Mean baseline left ventricular ejection fraction was $31 \pm 4\%$ and was reduced in 81% ($n=19$) of patients. On follow up, left ventricular ejection fraction normalized in 9 and remained depressed in 8 patients. Those patients with normal left ventricular ejection fraction at 6-8 month follow-up, all remained clinically normal at long-term follow-up. This was in contrast to the outcome of those patients with reduced left ventricular ejection fraction at 6-8 months of whom 2 died and 3 continued to have persistent left ventricular dilation and systolic dysfunction. In a subset of 13 patients, radionuclide left ventricular ejection fraction was measured at rest and following exercise at long term follow-up. This evaluation demonstrated an abnormal exercise left ventricular ejection fraction response in most cases including 7/9 patients with normal resting ejection fraction. This finding indicates that left ventricular functional reserve may remain impaired long after a bout of acute myocarditis despite apparent normal resting function.

4. CHAGASIC MYOCARDITIS AND CARDIOMYOPATHY

Echocardiography has evolved as an important modality in evaluating the cardiac status of patients with chagasic heart disease. During the earliest phase of an acute infection, two-dimensional and Doppler echocardiography may be normal. However, highly sensitive methods such as tissue Doppler imaging may reveal subtle abnormalities of the right ventricular systolic and diastolic function (26). Later during the acute infection, echocardiography reveals abnormal segmental left ventricular wall motion, most

commonly in the anterior and/or apical regions (27). The overall left ventricular size and ejection fraction is typically normal. Fatal acute myocarditis may occur in a minority (5-10%) of patients. The acute phase may be followed by a long indeterminate phase during which electrocardiographic or radiological abnormalities may not be detectable. A substantial number of these individuals (10-30%) will eventually evolve into the serious and potentially fatal chronic phase of the disease.

Early echocardiographic studies focused on evaluating patients with symptomatic advanced chagasic heart disease (28). The most typical finding in such individuals is an apical left ventricular aneurysm with or without thrombus, and/or basal inferoposterior hypokinesis or akinesis with preserved contractile function in the ventricular septum (28). The left atrium is often enlarged and the left ventricle is dilated with reduced systolic function. In cases of advanced cardiomyopathy with congestive heart failure, biventricular dilation occurs without increased wall thickness (eccentric hypertrophy). The segmental and global left ventricular dysfunction occurs in the absence of epicardial coronary artery disease. Although a number of studies have demonstrated an overall good prognosis for patients in the indeterminate phase of chagasic heart disease, in at least one area 2 to 5% of patients progress annually into the chronic phase and some patients may die suddenly (28). Therefore, identification of occult cardiac dysfunction may be of clinical significance for risk stratification. Cardiac abnormalities have been demonstrated in autopsy specimens or by endomyocardial biopsy in those with no apparent cardiomyopathy on noninvasive testing. Pathological findings have included carditis, focal inflammatory infiltration, myocytolysis and altered interstitial collagen matrix.

Cardiac structural and functional alterations are detectable in some patients in the indeterminate phase of chagasic heart disease, when sensitive methods of assessment are used such as treadmill exercise testing, high resolution and dynamic electrocardiography, noninvasive autonomic nervous system evaluation, radioisotope ventriculography and echocardiography. The goal of such studies is to identify prospectively *Trypanosoma cruzi*-infected persons who are at an increased risk of sudden death or progression to the chronic symptomatic phase. Abnormalities of left ventricular contraction and relaxation have been demonstrated on simultaneous phonocardiography, apexcardiography and echocardiography in asymptomatic patients with positive serology, without evidence of cardiac disease. Employing pulsed-wave and tissue Doppler imaging techniques, a recent study identified an abnormally prolonged isovolumic relaxation time and deceleration time of the early transmitral flow (29). In addition, the isovolumic contraction time was prolonged in the ventricular septal myocardium. These observations indicate that subtle abnormalities of both diastolic and systolic left ventricular function are present in the indeterminate phase.

Further support for the presence of occult left ventricular dysfunction has been presented by a study using

dobutamine stress echocardiography to evaluate contractile reserve in patients with and without resting wall motion abnormality (30). Neither group of patients reached target heart rate during dobutamine infusion, a finding indicative of chronotropic incompetence. In addition, both groups of patients exhibited a blunted contractile response to inotropic stimulation. Thus, compared with a normal value of 67%, the fractional left ventricular area change was only 50% in those with normal and 30% in those with abnormal resting wall motion. A biphasic segmental wall motion, defined as an initial improvement followed by deterioration at higher doses of dobutamine, was only seen in individuals with abnormal left ventricular wall motion at baseline (30). The latter was most commonly seen in the mid-posterior or posteroinferior left ventricular regions. All patients had normal epicardial coronary arteries by angiography. This may reflect abnormalities in coronary flow reserve due to microcirculatory dysfunction. In fact, impaired endothelial-dependent coronary vasodilation has been demonstrated in those with normal coronary arteries on angiography. Myocardial perfusion defects have been shown by thallium-201 scintigraphy in individuals with Chagas disease without apparent cardiac involvement. These perfusion abnormalities closely parallel those of (I-123)-meta-iodobenzoguanidine (MIBG) scintigraphic findings used for evaluation of cardiac sympathetic innervation (31). Regional myocardial ischemia, or inflammation, or both, may be responsible for these scintigraphic abnormalities.

Prognostic information has been provided by echocardiography in patients with established chagasic heart disease. In this regard, both left ventricular size and systolic function have been found to predict short-term prognosis. The prognosis of cardiomyopathy has also been found to be worse than that for other etiologies of left ventricular systolic dysfunction. This is attributed to the presence of an apical aneurysm that alters the normal prolate-ellipsoid shape of the left ventricle and has a potential for producing arrhythmias, thromboembolic events, or congestive heart failure (32). More recently, cardiac magnetic resonance imaging has been used in the evaluation of patients with chagasic heart disease and may prove to be a useful adjunct (33). Myocardial inflammation can also be detected by means of gallium-67 myocardial scintigraphy and tissue characterization using magnetic resonance imaging with contrast.

5. BACTERIAL MYOCARDITIS

The common causative agents of bacterial myocarditis are listed in Table 1. The hallmark of myocardial infections caused by these microorganisms is the development of microabscesses (Figure 3). The infection is spread to the myocardium during septicemia, coronary embolism of infected valvular vegetations from infective endocarditis (34,35), or from an adjacent focus of infection such as pneumonia, purulent pericarditis (36) and native or prosthetic heart valve endocarditis (37) (Figure 4). When myocardial abscess complicates native valve endocarditis, the causative organism is often staphylococcus and the valve involved is the aortic.

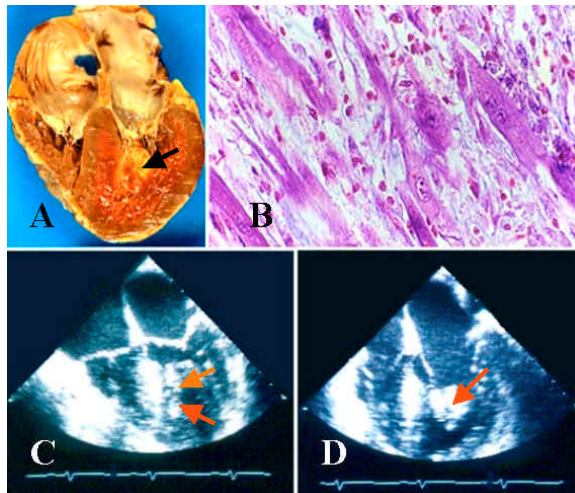


Figure 3. Coronal section of the heart (A) of a 44-year old woman with diabetes mellitus and staphylococcal sepsis showing a large myocardial abscess adjacent to the posteromedial papillary muscle (arrow). The abscess can also be seen on the end-systolic (C) and diastolic (D) still frames obtained from transesophageal echocardiographic study performed shortly before death (arrows). Inflammatory infiltration and myocyte necrosis are evident on histology (B, hematoxylin & eosin).

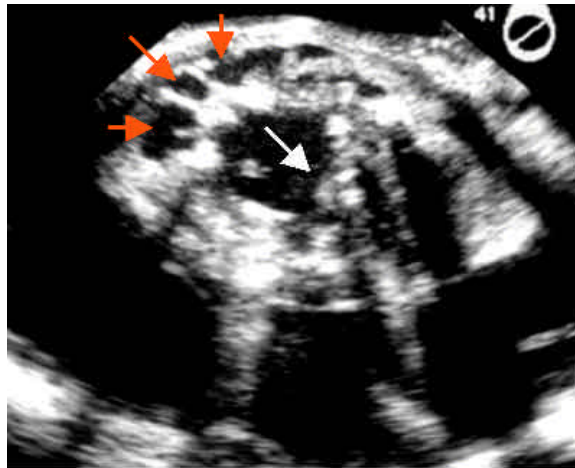


Figure 4. Transesophageal echocardiographic image of a mechanical prosthesis in aortic valve position demonstrating extensive tissue destruction and abscess formation (shown as echolucent pouches) in the perivalvular region (red arrows). Irregularly shaped infective vegetations are also present on the sewing ring and protrude into the prosthetic orifice (white arrow).

Endocarditis of a heavily calcified aortic valve is more likely to spread to the perivalvular tissue.

Bacteremia during the early phase of an acute myocardial infarction may also result in infection and abscess formation within the necrotic myocardium (38,39). Transmural involvement of the left ventricular wall by myocardial abscess may result in free wall rupture (35) or to formation of a pseudoaneurysm (36). In the past, most

myocardial abscesses were identified at necropsy. However, antemortem detection of myocardial abscess is increasingly made with the use of noninvasive imaging techniques including transthoracic (40) and transesophageal echocardiography, magnetic resonance imaging (41), computerized tomography, and indium-111 labeled white blood cell imaging (42). To perform the latter, roughly 60 milliliters of venous blood is drawn from the patient and mixed with an anticoagulant solution. The white blood cells are separated and labeled with the radioactive isotope, centrifuged, resuspended in isotonic sodium chloride solution, and reinjected into the patient. The injected radioactive leukocytes will then accumulate in the areas of inflammation or abscess. Images are obtained with a gamma-ray camera within 18-24 hours.

6. ACQUIRED IMMUNODEFICIENCY SYNDROME

Infection with human immunodeficiency virus and the resultant immunodeficiency syndrome is associated with a number of cardiac complications including myocarditis. The latter is often clinically silent and is identified by echocardiography in otherwise asymptomatic patients (43,44) or at necropsy as focal nonspecific lymphocytic infiltration (45). A specific etiology for myocarditis is not often found, although a small percentage may be caused by opportunistic pathogens such as *Toxoplasma gondii*, *Mycobacterium tuberculosis*, *Cryptococcus neoformis*, other fungi, or viruses. Other etiologies of left ventricular dysfunction include use of illicit drugs, cardiotoxic side effects of pharmacologic agents, neoplastic infiltration of the heart. Regardless of the underlying etiology, left ventricular dysfunction in patients with acquired immunodeficiency syndrome is characterized by cardiomegaly on chest roentgenogram and increased left ventricular dimensions and reduced ejection fraction by echocardiography. Associated functional mitral regurgitation, pulmonary hypertension and pericardial effusion are often detected by echocardiography. A direct relationship has been observed between left ventricular dysfunction and severity of immunodeficiency as measured by the CD4 count (46). Patients with irreversible left ventricular dysfunction have a mean survival of 101 days as a result of complications of heart failure or the underlying advanced immunodeficiency (47).

7. PERIPARTUM CARDIOMYOPATHY

Heart failure develops in the last months of pregnancy or within 5 months of delivery in about 1 in every 3,000 live births in the United States (48). This accounts for 1,500 new instances of peripartum cardiomyopathy each year (49). In such patients, by definition, an identifiable cause for the heart failure is absent and patients have no recognizable prior heart disease (50). Peripartum cardiomyopathy likely has multiple etiologies. However, in a certain percentage of patients the disease is caused by viral myocarditis, either as a primary infection or as an activation of a previous subclinical infection due to relative immunologic suppression of pregnancy (16,51). Peripartum cardiomyopathy presents clinically with the symptoms and signs of congestive heart

Imaging in myocarditis

failure and may be complicated by ventricular arrhythmias, systemic embolism, atrioventricular valve regurgitation and pulmonary hypertension.

Echocardiography is the standard diagnostic test for peripartum cardiomyopathy. Findings include increased left ventricular diastolic dimension and decreased ejection fraction. Left atrial enlargement and mitral regurgitation are frequently seen. In addition to diagnosis, echocardiography can be used to exclude other cardiovascular causes of heart failure in the pregnant women, screen family members to exclude a genetic predisposition to cardiomyopathy, monitor response to therapy (52), or evaluate postpartum recovery of left ventricular function (53-56). Echocardiography has demonstrated complete postpartum recovery of left ventricular function in 15% to 50% of women with peripartum cardiomyopathy. However, despite complete recovery of resting function, left ventricles of patients with peripartum cardiomyopathy may suboptimally respond to inotropic challenge during dobutamine stress echocardiography (57). This may explain the continued risk of recurrence of heart failure during subsequent pregnancy in some patients with peripartum cardiomyopathy and apparent complete recovery of left ventricular function (58).

8. CARDIAC IMAGING IN EXPERIMENTAL MODELS OF MYOCARDITIS

Animal models of infectious myocarditis have been developed in order to elucidate the pathophysiologic mechanisms involved in disease onset and progression. More recently, transgenic overexpressor and null mice have been created, and infected with various agents, in an effort to further explore the molecular basis of infectious myocarditis, thus targeting the role of a specific gene and/or gene product in the disease process. Initial attempts at understanding the hemodynamic and physiologic alterations in cardiovascular function depended on invasive, catheter-based approaches. Such studies have the advantage of providing detailed, reliable physiologic data, including measurements of intracardiac pressures, cardiac output and other measures of myocardial contraction, relaxation and overall performance, under controlled conditions (59). Catheter-based studies are, however, limited by the fact that the invasive and traumatic nature of the study precludes serial examinations. Other techniques such as radiolabelled microsphere and indicator dilution are technically demanding and provide limited and indirect data (60). Cardiac noninvasive assessment, using echocardiography and magnetic resonance imaging, however, can be performed repetitively with minimal, if any, trauma to the animal. These noninvasive evaluations have now become an integral part of studies seeking to determine the compensatory physiologic cardiovascular responses to myocardial infection in small animals (61).

8.1. Echocardiography

Transthoracic echocardiography has been used in several animal models of infectious myocarditis including those caused by coxsackie B virus, adenovirus, coronavirus, cytomegalovirus, and *Trypanosoma cruzi* (62-65). Animals studied have included dogs, pigs, and

monkeys (64-67). These studies have proved useful for evaluation of the type, extent and time course of development of cardiac anatomic abnormalities within the natural course of infectious myocarditis and have helped elucidate the mechanisms underlying the cardiac involvement in this disease.

With the advent of high frequency, small footprint transducers, it has become feasible to perform echocardiographic studies of smaller animals (68,69). Left and right ventricular and atrial alterations have been quantified and compared over time and the resultant cardiomyopathy has been characterized in regards to cardiac structure and function by serial comparisons between non-transgenic infected and uninfected (control) littermates. Comparison of infected transgenic and non-transgenic siblings has made possible the assessment of the relative contribution of a specific molecular derangement to the development of cardiomyopathy. Response to treatment has similarly been evaluated.

Transthoracic echocardiography in small animals is generally performed with the animal in a supine position on a heating pad set at 38°C (69). Anesthesia is achieved either by inhalation (e.g. Isoflurane), or by intraperitoneal injection (e.g. chloral hydrate) (69). M-mode and two-dimensional studies are performed using high frequency transducers with high resolution. Using the high temporal resolution of M-mode echocardiography, left ventricular size and systolic function can be accurately assessed despite the rapid heart rate of the small animal. Left ventricular measurements include the end-diastolic and end-systolic diameters, as well as the thickness of the ventricular septum and posterior wall. Additionally, the right ventricular size can be assessed on two-dimensional views of the heart. Left ventricular diastolic function has been assessed by the use of spectral and color-M-mode Doppler in genetically altered mice (70). Several studies have used the information obtained by transthoracic echocardiography to assess the relative contributions of a wide range of factors such as cytokines, inducible nitric oxide and endothelin to the development of specific etiologies of infectious myocarditis (71, 72). Other studies have evaluated the effects of various treatment modalities on the time course of the development and progression of myocarditis (73, 74).

Echocardiographic assessment of cardiac physiology offers several advantages over invasive techniques. First, it may be performed quickly, at low cost, and serially in the same animal. Second, invasive procedures require the administration of anesthetic agents. None of the currently available anesthetic agents are without significant cardiac effects in small animals such as mice, resulting in an abnormal baseline physiologic assessment. For example, the normal resting heart rate of a mouse ranges between 500-650 beats per minute. However the typical heart rates utilized during invasive hemodynamic studies range from 250-400 beats per minute. Left ventricular ejection fraction is also reduced under these conditions. Echocardiography has been successfully performed in non-anesthetized trained animals, lightly sedated animals, and awakened mice after recovery

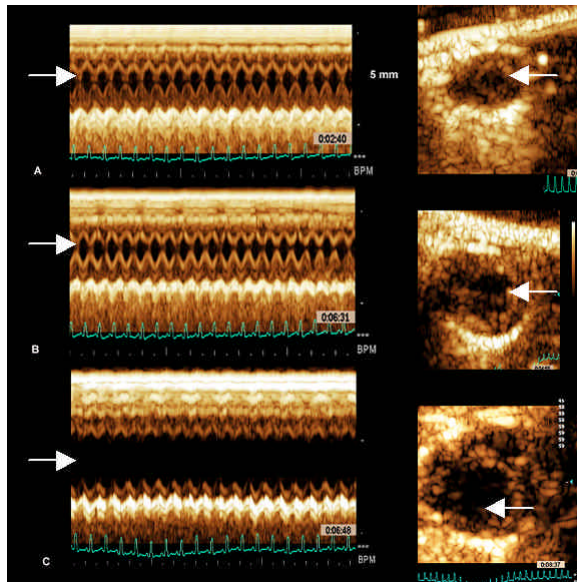


Figure 5. M-mode (left panels) and two-dimensional (right panels) images of the hearts of normal uninfected (A) mouse and those of mice infected with *Trypanosoma cruzi* with intermediate (B) or severe (C) degrees of left ventricular dilation and systolic dysfunction. Arrows to point to the left ventricular cavity.

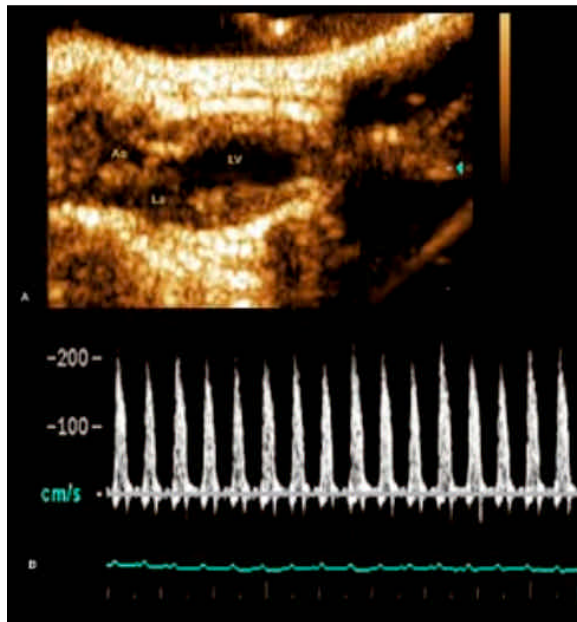


Figure 6. Two-dimensional transthoracic longitudinal view of the heart in a mouse showing the left ventricular (LV) cavity, left atrium (LA) and the ascending aorta (AO) to the left of a closed aortic valve. Pulsed-wave Doppler spectral display of the left ventricular outflow tract is shown at the bottom.

from light anesthesia, all at normal resting heart rates (69, 73,75). Preliminary results have been encouraging for the use of contrast (76, 77) and transesophageal (78,79) echocardiography for the assessment of myocardial perfusion and right ventricular function in small animals.

There is an inherent limitation to any methodology used for the in vivo assessment of cardiac physiology. All currently known indexes of in vivo cardiac systolic and diastolic function are load-dependant to various degrees. Currently, echocardiographic methods are not available to directly assess loading conditions. Similarly, cardiac myocyte contractility and diastolic function cannot be directly assessed. These factors may result in differences in serial measurements on the basis of altered loading conditions rather than a true physiologic change in cardiac performance.

8.1.1. *Trypanosoma cruzi* infection in murine models

The evaluation of the consequences of *Trypanosoma cruzi* infection in mice has been the focus of attention for many decades. The ultimate fate of this infection in the mouse is dependent on the strain of mouse as well as the strain of the parasite (80). For example, infection with the cardiomyopathic strain of *Trypanosoma cruzi* (Brazil strain) results in a 60-70% mortality in CD1 (outbred) mice by days 35-40 post infection (81). Intense inflammation, myonecrosis, myocytolysis, vasculitis and numerous parasite pseudocysts characterize acute chagasic myocarditis. Chronic inflammation and fibrosis characterize chronic murine chagasic cardiomyopathy, which evolves over a period of approximately 3 months. C57BL/6 mice similarly infected with the Brazil strain do not die acutely but rather develop a chronic cardiomyopathy by 3-6 months post-infection (82). Among the first abnormalities evident by echocardiography, at approximately 3 months post-infection, is dilation of the right ventricle (83). Thereafter, progressive right and left ventricular dilation, wall thinning and systolic dysfunction, as determined by ejection fraction measurements, are all prominent features in the subsequent 3 months post-infection (74) (Figure 5). In contrast, C57BL/6 mice infected with the reticulotropic Tulahuen strain die rapidly by 18-25 days post-infection with a significant parasitemia and a fulminate myocarditis characterized by the rapid development of right and left ventricular abnormalities as early as 10 days post-infection (69). Chagasic heart disease is also accompanied by vasculopathy (69, 82) manifested by microvascular spasm and decreased blood flow (82).

Myocardial injury resulting from *Trypanosoma cruzi* infection activates several signaling pathways including those involved in NF- κ B, vascular adhesion molecules, TGF- β , endothelin, kinins (71, 82, 84, 85) and the mitogen activated protein kinases (86). The induction of inflammatory mediators such as inducible nitric oxide synthase may have both beneficial and deleterious effects. For example, nitric oxide generated from inducible nitric oxide synthase is required for parasite killing but can also contribute to depression of left ventricular function. Thus, Brazil strain infected inducible nitric oxide synthase null mice demonstrate less ventricular dilation and systolic dysfunction compared to infected wild type mice (83, 87).

8.1.2. Future direction

Advances in transducer design and increasing processing speed will improve the quantitative echocardiographic assessment of cardiac physiology in very small animals. Doppler cardiographic estimation of stroke volume through assessment of aortic or pulmonic waveforms is feasible and may prove useful (Figure 6). Improved

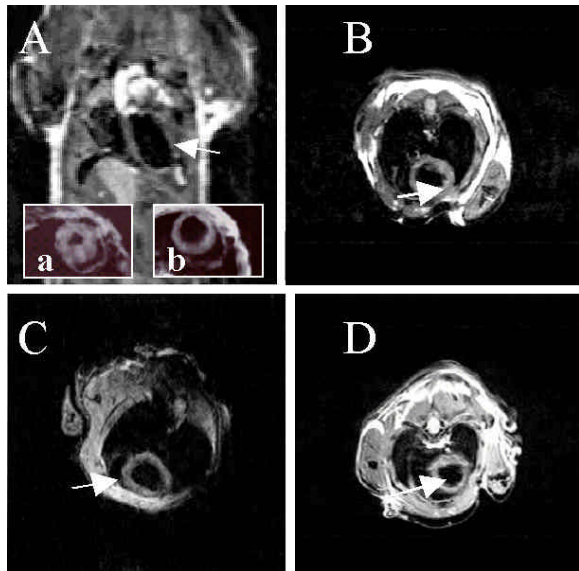


Figure 7. Magnetic resonance imaging in mice. Panel A shows a long axis oblique image; the white arrow indicates the left ventricle. The inset a shows a short axis image positioned at mid ventricle of a mouse heart in systole and b shows the same heart in diastole. Panel B shows a diastolic short axis image of a wild type mouse heart. Panels C and D show diastolic short axis images of mice infected with Tulahuen (C) and Brazil (D) strains of *Trypanosoma cruzi*. The white arrows in panels B, C, and D indicate the right ventricle. Note the dilated right ventricular chamber in the mouse infected with Brazil strain and the dilated left ventricular chamber in the mouse infected with the Tulahuen strain.

processing speed may also make color Doppler assessment of valvular lesions possible in these small animals with fast heart rates (61).

8.2. Magnetic Resonance Imaging

The application of magnetic resonance imaging to the study of small animal models of cardiac disease, while challenging, has yielded promising results (72, 74, and 87-108). This noninvasive study provides accurate, serial, three-dimensional images of the heart and has been used in the evaluation of several murine models of inflammatory and infectious myocarditis including acute and chronic *Trypanosoma cruzi* infection (71, 72, 74, 82, 87, 88) and other studies related to the inflammatory response in mice over-expressing tumor necrosis factor (89-91).

8.2.1. *Trypanosoma cruzi* infection

Magnetic resonance imaging studies of experimental Chagas' disease have included the evaluation of acute and chronic infections and assessment of pharmacologic interventions in wild type, transgenic and null mice (Figure 7).

Early studies of *Trypanosoma cruzi*-infected C57/BL/6 X 129sv (wild type) mice revealed enlargement of the right ventricle (71, 87). Thus, infected wild type mice exhibit almost doubling of the internal diameter of the right ventricle. This early cardiac effect of infection with

Trypanosoma cruzi was ameliorated in inducible nitric oxide synthase null mice (71). Therefore, inducible nitric oxide synthase null mice exhibited significantly less right ventricular dilation (1.4 fold). The findings support the hypothesis that nitric oxide derived from inducible nitric oxide synthase, released during acute infection, is involved in the cardiac remodeling in chronic experimental Chagas' disease.

Verapamil, a calcium channel blocker that has no direct effect on the parasite, also reduces the degree of right ventricular dilation (71, 73). Verapamil ameliorates the infection-associated inflammatory response and reduces the expression of cytokines. This may be responsible for the amelioration of cardiac pathology in chronically infected mice by verapamil.

Endothelin-1 is also upregulated during acute infection with *Trypanosoma cruzi*. Endothelin-1 has numerous physiological effects (72, 82) and is a proinflammatory molecule. Endothelin-1 null mice do not survive; however, mice in whom the gene for endothelin-1 is selectively deleted cardiac myocytes are viable. Magnetic resonance imaging studies of these mice infected with *Trypanosoma cruzi* demonstrate amelioration of the right ventricular remodeling observed in other mouse strains. This finding suggests that endothelin-1 is another important factor in the pathogenesis of chagasic heart disease. Further evidence for the role for endothelin-1 comes from studies using phosphoramidon (74, 88). Phosphoramidon is a type II integral membrane bound metalloproteinase and is a dual inhibitor of endothelin converting enzyme (required for processing active endothelin-1) and neutral endopeptidase. Phosphoramidon treatment of infected mice resulted in significantly reduced right ventricular remodeling, pathology, and mortality. In fact, phosphoramidon treated infected mice did not die acutely, whereas untreated infected mice had a mortality of up to 70% during the acute stage of infection.

Gamma interferon is a cytokine involved in natural resistance against parasitic infections through the induction of guanine triphosphatases (e.g. IGTP) (101). Recent magnetic resonance imaging studies of mice deficient in IGTP suggests that it also play a role in right ventricular remodeling during *Trypanosoma cruzi* infection.

8.2.2. Tumor necrosis factor

Over the past several years, studies of mice over-expressing the cytokine tumor necrosis factor- α have been reported (89-91). Tumor necrosis factor- α expression is increased in heart failure, various infections and in the sepsis syndrome. Mice over-expressing tumor necrosis factor- α in the heart at various levels have been examined by magnetic resonance imaging. Tumor necrosis factor- α over-expressor mice exhibit increased heart/body weight and myocarditis. Magnetic resonance imaging of these mice revealed dilation of both ventricles and reduced ejection fraction. The cardiac pathology worsens with age and with increased levels of tumor necrosis factor- α expression. The results provide evidence that cardiac inflammation can evolve to a dilated cardiomyopathy, with tumor necrosis factor- α being an important mediator of both processes.

8.2.3. Future direction

To date, most cardiac magnetic resonance imaging studies of the small animals have focused on the morphology, particularly that of the left ventricle. With recent advances in technology and analysis tools these studies can now be expanded to application involving evaluation of bioenergetics, regional wall motion and wall thickening, as well as the right ventricular function.

Myocardial high-energy phosphates (adenosine triphosphate and phosphocreatine) can be non-invasively quantified by ^{31}P magnetic resonance spectroscopy in conjunction with magnetic resonance imaging used to guide the spectroscopic studies. Cardiac phosphocreatine to adenosine triphosphate ratio is altered during chronic heart failure. Rats infected with *Trypanosoma cruzi* exhibit energy impairment at the mitochondrial level (102). It is likely that a similar impairment of cardiac bioenergetics exists in infected mice and humans. Using a ^{31}P surface coil and ^1H imaging body coil both morphological and biochemical information can be acquired during the same imaging experiment. The noninvasive nature of these methods makes them attractive tools for serial evaluation of cardiac structure and function and for evaluation of therapeutic interventions. Although very few *in vivo* ^{31}P magnetic resonance spectroscopic studies of mice have been reported the technique has been elegantly applied in recent studies (103, 104).

Evaluation of wall motion and wall thickening is another area for future studies (98, 105, 106). Methods include myocardial tagging (105) and development of image analysis tools. Tagging studies in normal mice have demonstrated that left ventricular torsion in mice is similar to that of the human (105). Challenges with this method include those that apply to routine imaging such as small heart size and rapid heart rate of the small animal, and other factors such as the requirement for advanced image analysis and specific pulse sequences. This area of research may be especially useful for the complete characterization of murine cardiovascular performance. Simpler methods for analysis of wall motion and thickening using centerline analysis may prove more readily accessible and easier to implement since routine images acquired with simpler sequences such as FLASH and spin-echo, can be analyzed. Issues with these methods involve automation of border detection and segmentation to reduce the time required for analysis.

Detailed evaluation of right ventricular wall thickness and function has been more challenging than the study of the left ventricle in mice. The right ventricular wall is much thinner (~ 0.5 mm) than that of the left ventricle (~ 1.0 mm) and is likely to be at the limits of the resolution of most routine *in vivo* magnetic resonance images. Recently, Wiesmann *et al.* (107) reported a study of right ventricular function in mice using magnetic resonance imaging. Murine right ventricular end-diastolic and end-systolic volumes were significantly increased compared with left ventricular volumes. In a preliminary report, right ventricular wall thickening has been evaluated using a centerline approach (108) similar to that described

for the evaluation of the left ventricular wall thickening (98).

9. CONCLUSIONS

Noninvasive cardiac imaging in clinical and experimental myocarditis has evolved rapidly over the last two decades. It has allowed serial assessment of cardiovascular structure and function without the general disadvantages of invasive studies. The most important clinical contribution of noninvasive cardiac imaging may be in making the diagnosis of the disease without a need for endomyocardial biopsy and in predicting the outcome of the disease. Experimentally, cardiac imaging has provided complementary data to invasive and histomorphologic, biochemical and molecular studies. Noninvasive cardiac imaging has been instrumental in the assessment of the natural history of experimental myocarditis. Further technical developments in cardiac imaging will allow more detailed evaluation of acute myocarditis in humans and in animals.

10. ACKNOWLEDGEMENTS

We wish to thank Ms. Nyasia Lloyd, Division of Cardiology, Montefiore Medical Center, for her assistance in preparation of this manuscript. This work was supported by grants from the NIH and the American Heart Association (HBT).

11. REFERENCES

1. Nieminen M.S., J. Heikkilä, & J. Karjalainen: Echocardiography in acute infectious myocarditis: relation to clinical and electrocardiographic findings. *Am J Cardiol* 53, 1331-1337 (1984)
2. Pinamonti B, E. Alberti, A. Cigalotto, L. Dreas, A. Salvi, F. Silvestri & F. Camerini: Echocardiographic findings in myocarditis. *Am J Cardiol* 62, 285-291 (1988)
3. Felker G.M., J.P. Boehmer, R.H. Hruban, G.M. Hutchins, E.K. Kasper, K.L. Baughman & J.W. Hare: Echocardiographic findings in fulminant and acute myocarditis. *J Am Coll Cardiol* 36, 227-232 (2000)
4. Hauser A.M., S. Gordon, J. Cieszkowski & G.C. Timmis: Severe transient left ventricular "hypertrophy" occurring during acute myocarditis. *Chest* 83, 275-277 (1983)
5. Dec G.W., Jr., I.F. Palacios & J.T. Fallon: Cardiomyopathies. Clinical features, histologic correlates, and clinical outcome. *N Engl J Med* 312, 885-890 (1985)
6. Chandraratna P.A., A. Nimalasuriya, C.L. Reid, S. Cohn & S.H. Rahimtoola: Left ventricular asynergy in acute myocarditis. Simulation of acute myocardial infarction. *J Am Med Assoc* 250, 1428-1430 (1983)
7. Ikaheimo M.J. & J.T. Takkunen: Echocardiography in acute infectious myocarditis. *Chest* 89, 100-102 (1986)
8. Van Dam J, F.C. Basilio & R.W. Nesto: Echocardiography in acute myocarditis associated with left ventricular thrombus formation and systemic embolization. *J Ultrasound Med* 9, 599-602 (1990)
9. Kimball T.R., S.A. Witt, L.A. Marasco, C.J. Bushman, D.C. Schwartz & E.T. Ballard: A unique echocardiographic

presentation of acute myocarditis: restrictive pathophysiology. *J Am Soc Echocardiogr* 7,187-189 (1994)

10. Leiback E, I. Hardouin, R. Meyer, J. Bellach & R. Hetzer: Clinical value of echocardiographic tissue characterization in the diagnosis of myocarditis. *Eur Heart J* 17,135-142 (1996)

11. Di Cesare E. MRI of the cardiomyopathies. *Eur J Radiol* 38,179-184 (2001)

12. Chandraratna, P.A., W.G. Bradley, K.E. Kortman, S. Minagoe, M. Delvicario & S.H. Rahimtoola: Detection of acute myocarditis using nuclear magnetic resonance imaging. *Am J Med* 83,1144-1146 (1987)

13. Gagliardi MG., M. Bevilacqua, P. Di Renzi, S. Picardo, R. Passariello & C. Marcelletti. Usefulness of magnetic resonance imaging for diagnosis of acute myocarditis in infants and children, and comparison with endomyocardial biopsy. *Am J Cardiol* 68,1089-1091 (1991)

14. Friedrich M.G., O. Strohm, J. Schulz-Menger, H. Marciniak F.C. Luft & R. Dietz: Contrast meia-enhanced magnetic resonance imaging visualizes myocardial changes in the course of viral myocarditis. *Circulation* 97,1802-1809 (1998)

15. O'Connell J.B., J.A. Robinson, R.E. Henkin & R.M. Gunnar: Immunosuppressive therapy in patients with congestive cardiomyopathy and myocardial uptake of gallium-67. *Circulation* 64, 780-786 (1981)

16. O'Connell J.B., M.R. Costanzo-Nordin, R. Subramanian, J.A. Robinson, D.E. Wallis, P.J. Scanlon & R.M. Gunnar: Peripartum cardiomyopathy: clinical, hemodynamic, histologic and prognostic characteristics. *J Am Coll Cardiol* 8, 52-56 (1986)

17. Shulkin B.I. & R.L. Wahl. SPECT imaging of myocarditis. *Clin Nucl Med* 12, 841-842 (1987)

18. Narula J., B.A. Khaw, G.W. Dec Jr, I.F. Palacios, J.F. Southern, J.T. Fallon, H.W. Strauss, E. Haber & T. Yasuda: Brief report: recognition of acute myocarditis masquerading as acute myocardial infarction. *N Engl J Med* 328, 100-104 (1993)

19. Matsuura H, I.F. Palacios, G.W. Dec, J.T. Fallon, H. Garan, J.N. Ruskin & T. Yasuda: Intraventricular conduction abnormalities in patients with clinically suspected myocarditis are associated with myocardial necrosis. *Am Heart J* 127, 1290-1297 (1994)

20. Dec G.W., I. Palacios, T. Yasuda, J.T. Fallon, B.A. Khaw, H.W. Strauss & E. Haber: Antimyosin antibody, cardiac imaging: its role in the diagnosis of myocarditis. *J Am Coll Cardiol* 16, 97-104 (1990)

21. Casans I, A. Villar, V. Almenar & A. Blanes: Lyme myocarditis diagnosed by indium-111-antimyosin antibody scintigraphy. *Eur J Nucl Med* 15, 330-331 (1989)

22. Ballester M, D. Obrador, I. Carrió, C. Moya, J.M. Augé, R. Bordes, V. Martí, I. Bosch, I. Bernà-Roqueta, M. Estorch, G. Pons-Lladó, M.L. Càmar, J.M. Padró, A. Arís & J.M. Caralps-Riera: Early postoperative reduction of monoclonal antimyosin antibody uptake is associated with absent rejection-related complications after heart transplantation. *Circulation* 85, 62-68 (1992)

23. Carrió I, A. Lopez-Pousa, M. Estorch, D. Duncker, L. Berna, G. Torres & L. de Andres: Detection of doxorubicin cardiotoxicity in patients with sarcomas by

indium-111-antimyosin monoclonal antibody studies. *J Nucl Med* 34, 1503-1507 (1993)

24. Ballester M., V. Martí, I. Carrió, D. Obrador, C. Moya, G. Pons-Llado, L. Berna, R. Lamich, M.R. Aymar, M. Barbanój, J. Guardia, F. Carreras, C. Udina, J.M. Auge, J. Marrugat, G. Permanyer & J.M. Caralps-Riera: Spectrum of alcohol-induced myocardial damage detected by indium-111-labeled monoclonal antimyosin antibodies. *J Am Coll Cardiol* 29, 160-167 (1997)

25. Quigley P.J., P.J. Richardson, B.T. Meany, E.G.J. Olsen, M.J. Monaghan, G. Jackson & D.E. Jewitt: Long-term follow-up of acute myocarditis. Correlation of ventricular function and outcome. *Eur Heart J* 8(suppl J), 39-42 (1987)

26. Barros M.V.L., F.S. Machado, A.L.P. Ribeiro & M.O.C. Rocha: Detection of early right ventricular dysfunction in Chagas' disease using Doppler tissue imaging. *J Am Soc Echocardiogr* 15, 1197-1201 (2002)

27. Parada H., H. Carrasco, N. Anez, C. Fuenmayor, & I. Inglessis: Cardiac involvement is a constant finding in acute Chagas disease: a clinical, parasitological and histopathological study. *Int J Cardiol* 60, 49-54 (1997)

28. Acquatella H, N.B. Schiller, J.J. Puigbo, H. Giordano, J.A. Suarez, H. Casal, N. Arreaza, R. Valecillos & E. Hirschhaut: M-mode and two-dimensional echocardiography in chronic Chagas heart disease: a clinical and pathologic study. *Circulation* 62, 787-799 (1980)

29. Barros M.V.L., M.O.C. Rocha, A.L.P. Ribeiro & F.S. Machado: Doppler tissue imaging to evaluate early myocardium damage in patients with undetermined form of Chagas disease and normal echocardiogram. *Echocardiography* 18, 131-136 (2001)

30. Acquatella H, J.E. Perez, J.A. Condado & I. Sanchez: Limited myocardial contractile reserve and chronotropic incompetence in patients with chronic Chagas disease. *J Am Coll Cardiol* 33, 522-529 (1999)

31. Simoes M.V., A.O. Pintya, G. Bromberg-Martin, A.V. Sarabanda, C.M. Antloga, A. Pazin-Filho, B.C. Maciel & J.A. Marin-Neto: Relation of regional sympathetic denervation and myocardial perfusion disturbance to wall motion impairment in Chagas cardiomyopathy. *Am J Cardiol* 86, 975-981 (2000)

32. Bestetti RB & G. Muccillo: Clinical course of Chagas heart disease: a comparison with dilated cardiomyopathy. *Int J Cardiol* 60, 187-193 (1997)

33. Kalil Filho R. & C.P. de Albuquerque: Magnetic resonance imaging in Chagas' heart disease. *Rev Paul Med* 113, 880-883 (1995)

34. Arita M., Y. Kusuyama, M. Takatsuji, K. Kawazoe & Y. Masuyama: Septal myocardial abscess and infectious pericarditis in a case of bacterial endocarditis. *Jpn Circ J* 49, 451-455 (1985)

35. Terry S.M. & P.E. Ryan Jr: Penetrating mitral valve annular abscess. *J Heart Valve Dis* 6, 621-624 (1997)

36. Roberts J.H., V. Aptone, D.P. Naidich & M. Bhalla: Myocardial abscess resulting in pseudoaneurysm: case report. *Cardiovasc Intervent Radiol* 14, 307-310 (1991)

37. Aguado J.M., F. Gonzalez-Vilchez, R. Martin-Duran, R. Arjona, J.A. Vazquez de Prada: Perivalvular abscesses associated with endocarditis. Clinical features and

diagnostic accuracy of two-dimensional echocardiography. *Chest* 104, 88-93 (1993)

38. Behnam R, S. Walter & V. Hanes: Myocardial abscess complicating myocardial infarction. *J Am Soc Echocardiogr* 8, 334-337 (1995)

39. Ghani M. & D. Boughner: Echocardiographic diagnosis of myocardial abscess complicating myocardial infarction. *J Am Soc Echocardiogr* 7, 318-320 (1994)

40. Wickline C.L., V.D. Goli, & J.C. Buell: Coronary artery narrowing due to extrinsic compression by myocardial abscess. *Cathet Cardiovasc Diagn* 23, 121-123 (1991)

41. Akins EW, R.M. Slone, B.N. Wiechmann, M. Browning, T.D. Martin & W.R. Mayfield: Perivalvular pseudoaneurysm complicating bacterial endocarditis: MR detection in five cases. *Am J Radiol* 156, 1155-1158 (1991)

42. Chakrabarti J: Diagnostic evaluation of myocardial abscesses. A new look at an old problem. *Int J Cardiol* 52,189-196.(1995)

43. Corallo S, M.R. Mutinelli, M. Moroni, A. Lazzarin, V. Celano, A. Repossini & G. Baroldi: Echocardiography detects myocardial damage in AIDS: prospective study in 102 patients. *Eur Heart J* 9, 887-892 (1988)

44. Akhras F., S. Dubrey, B. Gazzard & M.I. Noble: Emerging patterns of heart disease in HIV infected homosexual subjects with and without opportunistic infections: a prospective colour flow Doppler echocardiographic study. *Eur Heart J* 15, 68-75 (1994)

45. Baroldi G., S. Corallo, M. Moroni, A. Repossini, M.R. Mutinelli, A. Lazzarin, C.M. Antonacci, S. Cristina, C. Negri: Focal lymphocytic myocarditis in acquired immunodeficiency syndrome (AIDS): a correlative morphologic and clinical study in 26 consecutive fatal cases. *J Am Coll Cardiol* 12, 463-469 (1988)

46. Barbaro G, G. Di Lorenzo, B. Crisorio & G. Barbarini: Incidence of dilated cardiomyopathy and detection of HIV in myocardial cells of HIV-positive patients. Gruppo Italiano per lo Studio Cardiologico dei Pazienti Affetti da AIDS. *N Engl J Med* 339, 1093-1099 (1998)

47. R.A. Elton, R.P. Brettell & N.A. Boon: Heart muscle disease related to HIV infection: prognostic implications. *Brit Med J* 309, 1605-1607 (1994)

48. Demakis J.G., S.H. Rahimtoola, G.C. Sutton, W.R. Meadows, P.B. Szanto, J.R. Tobin & R.M. Gunnar: Natural course of peripartum cardiomyopathy. *Circulation* 44, 1053-1061(1971)

49. Ventura S.J., K.D. Peters, J.A. Martin & J.D. Maurer: Births and deaths: United States, 1996. *Mon Vital Stat Rep* 46, Suppl 2:1-40 (1997)

50. Pearson GD, Veille JC, Rahimtoola S, Hsia J, Oakley C.M., J.D. Hosenpud, A. Ansari & K.L. Baughman: Peripartum cardiomyopathy: National Heart, Lung, and Blood Institute and Office Rare Diseases (National Institutes of Health) workshop recommendations and review. *J Am Med Assoc* 283:1183-1189 (2000)

51. Felker G.M, C.J. Jaeger, E. Klodas, D.R. Thiemann, J.M. Hare, R.H. Hruban, E.K. Kasper, & K.L. Baughman: Myocarditis and long-term survival in peripartum cardiomyopathy. *Am J Heart* 140, 785-791 (2000)

52. Bozkurt B, F.S. Villaneuva, R. Holubkov, T. Tokarczyk, R.J. Alvarez Jr, G.A. MacGowan, S. Murali, W.D. Rosenblum, A.M. Feldman & D.M. McNamara:

Intravenous immune globulin in the therapy of peripartum cardiomyopathy. *J Am Coll Cardiol* 34, 177-180 (1999)

53. Elkayam U, P.P. Tummala, K. Rao, M.W. Akhter, I.S. Karaalp, O.R. Wani, A. Hameed, I. Gviazda & A. Shotan: Maternal and fetal outcomes of subsequent pregnancies in women with peripartum cardiomyopathy. *N Engl J Med* 344,1567-1571 (2000)

54. Ostrzega E. & U. Elkayam: Risk of subsequent pregnancy in women with a history of peripartum myopathy: results of a survey (abstract) *Circulation* 92, Suppl 1:I-333 (1995)

55. Albanesi Filho F.M.& T.T. da Silva: Natural course of subsequent pregnancy after peripartum cardiomyopathy. *Arg Bras Cardiol* 73:47-57 (1999)

56. Sutton M.S., P. Cole, M. Plappert, D. Saltzman, & S. Goldhaber: Effects of subsequent pregnancy on left ventricular function in peripartum myocardiopathy. *Am Heart J* 121, 1176-1178 (1991)

57. Lampert M.B., L. Weinert, J. Hibbard, C. Korcarz, M Lindheimer & R.M. Lang: Contractile reserve in patients with peripartum cardiomyopathy and recovered left ventricular function. *Am J Obstet Gynecol* 176,189-195 (1997)

58. Ceci O, C. Berardesca, F. Caradonna, P. Corsano, R. Guglielmi & L. Nappi: Recurrent peripartum cardiomyopathy. *Eur J Obstet Gynecol Reprod Biol* 76, 29-30 (1998)

59. Lorenz J.N. & J. Robbins: Measurement of intraventricular pressure and cardiac performance in the intact closed-chest anesthetized mouse. *Am J Physiol* 272: H1137-H1146 (1997)

60. Barbee R.W., B.D. Berry, R.N. Re & J.P. Murgoy: Microsphere and dilution techniques for the determination of blood flows and volumes in conscious mice. *Am J Physiol* 263, R728-R733 (1992)

61. Hoit B.D: New approaches to phenotypic analysis in adult mice. *J Mol Cell Cardiol* 33, 27-35 (2000)

62. Alexander L.K., B.W. Keene & R.S. Baric: Echocardiographic changes following rabbit coronavirus infection. *Adv Exp Med Biol* 380, 113-115 (1995)

63. Barr S.C, R.M. Simpson, S.P. Schmidt, M.M Bunge, J.M. Authement & F. Lozano: Chronic dilatative myocarditis caused by *Trypanosoma cruzi* in two dogs. *J Am Vet Med Assoc* 195, 1237-1241 (1989)

64. Hoshino T., C. Kawai & M. Tokuda: Experimental coxsackie B viral myocarditis in cynomolgus monkeys. *Jpn Circ J* 47, 59-66 (1983)

65. Gwathney J.K, S. Nakao, P.C. Come, M.E. Goad, J.R. Serur, A.V. Als & W.H. Abelmann: An experimental model of acute and subacute viral myocarditis in the pig. *J Am Coll Cardiol* 19, 864-869 (1992)

66. Barr S.C., Holmes RA & T.R. Klei: Electrocardiographic and echocardiographic features of trypanosomiasis in dogs inoculated with North American *Trypanosoma cruzi* isolates. *Am J Vet Res* 2, 53:521-527 (1992)

67. Shannon R.P., M.A. Simon, M.A. Mathier, Y.J. Geng, S. Mankad & A.A. Lackner: Dilated cardiomyopathy associated with simian AIDS in nonhuman primates. *Circulation* 101, 185-193 (2000)

68. Freeman G.L., J.T. Colston, M. Zabalgottia & B. Chandrasekar: Contractile depression and expression of

- proinflammatory cytokines and iNOS in viral myocarditis. *Am J Physiol* 274, H249-H258 (1998)
69. Chandra M., H.B. Tanowitz, S.B. Petkova, H. Huang, L.M. Weiss, M. Wittner, S.M. Factor, V. Shtutin, L.A. Jelicks, J. Chan & J. Shirani: Significance of inducible nitric oxide synthase in acute myocarditis caused by *Trypanosoma cruzi* (Tulahuen strain) *Int J Parasitol* 32, 897-905 (2002)
70. Schmidt A.G., M. Gerst, J. Zhai, A.N. Carr, L. Pater, E.G. Kranias & B. Hoit: Evaluation of left ventricular diastolic function from spectral and color M-mode Doppler in genetically altered mice. *J Am Soc Echocardiogr* 15, 1065-1073 (2002)
71. Huang H., J. Chan, M. Wittner, L.A. Jelicks, S.A. Morris, S.M. Factor, L.M. Weiss, V.L. Braunstein, C.J. Bacchi, N. Yarlett, M. Chandra, J. Shirani & H.B. Tanowitz: Expression of cardiac cytokines and inducible form of nitric oxide synthase (NOS2) in *Trypanosoma cruzi* infected mice. *J Mol Cell Cardiol* 31, 75-88 (1999)
72. Huang H., M. Yanagisawa, Y. Y. Kisanuki, L.A. Jelicks, M. Chandra, S.M. Factor, M. Wittner, L.M. Weiss, R.G. Pestell, V. Shtutin, J. Shirani & H.B. Tanowitz: Role of cardiac myocyte-derived endothelin-1 in chagasic cardiomyopathy: molecular genetic evidence. *Clin Sci* 103 (Suppl 1):263S-6S(2002)
73. Chandra M, J. Shirani, V. Shtutin, L.M. Weiss, S.M. Factor, S.B. Petkova, M. Rojkind, J.A. Dominguez-Rosales, L.A. Jelicks, M. Wittner, & H.B. Tanowitz: Cardioprotective effects of verapamil on myocardial structure and function in a murine model of chronic *Trypanosoma cruzi* infection (Brazil strain): An echocardiographic study. *Int J Parasitol* 32, 207-215 (2002)
74. Jelicks L.A., M. Chandra, J. Shirani, V. Shtutin, B. Tang, G.J. Christ, S.M. Factor, M. Wittner, H. Huang, L.M. Weiss, S. Mukherjee, B. Bouzahzah, S.B. Petkova, M.M. Teixeira, S.A. Douglas, M.L. Loreda, P. D'Orleans-Juste & H.B. Tanowitz: Cardioprotective effects of phosphoramidon on myocardial structure and function in murine Chagas' disease. *Int J Parasitol* 32, 1497-1506 (2002)
75. Yang X-P, Y-H Liu, N-E Rhaleb, N. Kurihara, H.E. Kim & O.A. Carretero: Echocardiographic assessment of cardiac function in conscious and anesthetized mice. *Am J Physiol* 277, H1967-H1974 (1999)
76. Mor-Avi V, C Korcarz, R. Fentzke, H. Lin, A.J. Leiden & R. Lang: Quantitative evaluation of left ventricular function in a transgenic mouse model of dilated cardiomyopathy with 2-dimensional contrast echocardiography *J Am Soc Echocardiogr* 12, 209-214 (1999)
77. Scherrer-Chosbie M, W. Steudel, R. Ulrich, P. Hunziker, N. Liel-Cohen, J. Newell, J. Zaroff, W. Zapol & M. Picard: Echocardiographic determination of risk area size in a murine model myocardial ischemia. *Am J Physiol* 277, H986-H992 (1999)
78. Scherrer-Chosbie M, W. Steudel, P. Hunziker, G. Foster, L. Garrido, M. Liel-Cohen, W. Zapol, & M. Picard: Determination of right ventricular structure and function to normoxic and hypoxic mice; a transesophageal echocardiographic study. *Circulation* 98, 1015-1021 (1998)
79. Steudel W, M. Scherrer-Crosbie, K. Bloch, J. Weimann, P. Huang, R. Jones, M. Picard & W. Zapol: Sustained pulmonary hypertension and right ventricular hypertrophy after chronic hypoxia in mice with congenital deficiency of nitric oxide synthase 3. *J Clin Invest* 101, 2468-2477 (1998)
80. Trischmann T, H.B. Tanowitz, M. Wittner & B. Bloom: *Trypanosoma cruzi*: The role of the immune response in the natural resistance of inbred strains of mice. *Exp Parasitol* 45, 160-166 (1978)
81. Tanowitz H.B., M. Wittner, B. Chen, H. Huang, L.M. Weiss, G.J. Christ, V.L. Braunstein, J.P. Bilezikian & S.A. Morris: Effects of Verapamil on acute Chagas' disease. *J Parasitol* 82, 814-819 (1996)
82. Petkova S.B., H. Huang, S.M. Factor, R.G. Pestell, B. Bouzahzah, L.A. Jelicks, L.M. Weiss, S.A. Douglas, M. Wittner & H.B. Tanowitz: The role of endothelin in the pathogenesis of Chagas' disease. *Int J Parasitol* 31, 499-511 (2001)
83. Rossi M: Microvascular changes as a cause of chronic cardiomyopathy in Chagas' disease. *Am Heart J* 120, 233-236 (1990)
84. Chandrasekar B, P.C. Melby, D.A. Troyer & G.L. Freeman: Differential regulation of nitric oxide synthase isoforms in experimental acute chagasic cardiomyopathy. *Clin Exp Immunol* 121, 112-119 (2000)
85. Tanowitz H.B., S.M. Factor, J. Shirani, A. Ilrcil, M. Wittner, J. Scharfstein & L.V. Kirchhoff: Recent developments in the pathology of Chagas disease with emphasis on the cardiovascular system. In: American Trypanosomiasis. Eds: Tyler K.M. & M.A. Miles, World Class Parasites (volume 7) Kluwer Academic Publishers: pp 81-96 (2002)
86. Huang H, S.B. Petkova, R.G. Pestell, B. Bouzahzah, J. Chan, H. Magazine, L.M. Weiss, G.J. Chris, M.P. Lisanti, S.A. Douglas, V. Shtutin, S.K. Halonen, M. Wittner & H.B. Tanowitz: *Trypanosoma cruzi* infection (Chagas' disease) of mice causes activation of the mitogen-activated protein kinase (MAPK) cascade and expression of endothelin-1 in the myocardium. *J Cardiovasc Pharmacol* 36, S148-S150 (2000)
87. Jelicks L.A., J. Shirani, M. Wittner, M. Chandra, L.M. Weiss, S.M. Factor, I. Bekirov, V.L. Braunstein, J. Chan, H. Huang & H.B. Tanowitz: Application of cardiac gated magnetic resonance imaging in murine Chagas' disease. *Am J Trop Med Hyg* 61, 207-214 (1996)
88. Jelicks L.A., M. Chandra, V. Shtutin, S.B. Petkova, B. Tang, G.J. Christ, S.M. Factor, M. Wittner, H. Huang, S.A. Douglas, L.M. Weiss, P.D. Orleans-Juste, J. Shirani & H.B. Tanowitz: . Phosphoramidon treatment improves the consequences of chagasic heart disease in mice. *Clin Sci* 103, 267S-271S (2002)
89. Franco F, G.D. Thomas, B. Giroir, D. Bryant, M.C. Bullock, M.C. Chwialkowski, R.G. Victor & R.M. Peshock: . Magnetic resonance imaging and invasive evaluation of development of heart failure in transgenic mice with myocardial expression of tumor necrosis factor-alpha. *Circulation* 99, 448-454 (1999)
90. Bryant D, L. Becker, J. Richardson, J. Shelton, F. Franco, R. Peshock, M. Thompson & B. Giroir: Cardiac failure in transgenic mice with myocardial expression of

- tumor necrosis factor- α . *Circulation* 97,1375-1381 (1998)
91. Kubota T, C.F. McTiernan, C.S. Frye, S.E. Slawson, B.H. Lemster, A.P. Koretsky, A.J. Demetris & A.M. Feldman: Dilated cardiomyopathy in transgenic mice with cardiac-specific overexpression of tumor necrosis factor- α . *Circ Res* 81, 627-635 (1997)
92. Siri F.M., L.A. Jelicks, L.A. Leinwand & J.A. Gardin: Gated magnetic resonance imaging of normal and hypertrophied murine hearts. *Am J Physiol* 272, H2394 - H2402 (1997)
93. Slawson S.E., B.B. Roman, D.S. Williams & A.P. Koretsky: Cardiac MRI of the normal and hypertrophied mouse heart. *Magn Reson Med* 39, 980-987 (1998)
94. Franco F, S.K. Dubois, R.M. Peshock & R.V. Shohet: Magnetic resonance imaging accurately estimates LV mass in a transgenic mouse model of cardiac hypertrophy. *Am J Physiol* 274, H679-H683 (1998)
95. Woodman S.E., D.S. Park, A.W. Cohen, M. Cheung, M. Chandra, J. Shirani, B. Tang, L.A. Jelicks, R.N. Kitsis, G.J. Christ, S.M. Factor, H.B. Tanowitz & M.P. Lisanti: Caveolin-3 knock-out mice develop a progressive cardiomyopathy and show hyperactivation of the p42/44 MAP kinase cascade. *J Biol Chem* 277, 38988-38997 (2002)
96. Park D.S., S.E. Woodman, W. Schubert, A.W. Cohen, P.G. Frank, M. Chandra, J. Shirani, B. Razani, B. Tang, L.A. Jelicks, S.M. Factor, L.M. Weiss, H.B. Tanowitz & M.P. Lisanti: Caveolin-1/3 double-knockout mice are viable, but lack both muscle and non-muscle caveolae, and develop a severe cardiomyopathic phenotype. *Am J Pathol* 160, 2207-2217 (2002)
97. Cohen A.W., D.S. Park, S.E. Woodman, T.M. Williams, M. Chandra, J. Shirani, A. Pereira De Souza, R.N. Kitsis, R.G. Russell, L.M. Weiss, B. Tang, L.A. Jelicks, S.M. Factor, V. Shtutin, H.B. Tanowitz & M.P. Lisanti MP: Caveolin-1-deficient mice develop cardiac hypertrophy and show hyper-activation of the p42/44 MAP kinase cascade in areas of interstitial fibrosis and isolated cardiac fibroblasts. *Am J Physiol Cell Physiol*. 2002 Oct 9 (epub ahead of print).
98. Williams S.P, H.P. Gerber, F.J. Giordano, F.V. Peale Jr, L.J. Bernstein, S. Bunting, K.R. Chien, N. Ferrara & N. van Bruggen: Dobutamine stress cine-MRI of cardiac function in the hearts of adult cardiomyocyte-specific VEGF knockout mice. *J Magn Reson Imaging* 14, 374-382 (2001)
99. Wiesmann F, J. Ruff, S. Engelhardt, L. Hein, C. Dienesch, A. Leupold, R. Illinger, A. Frydrychowicz, K.H. Hiller, E. Rommel, A. Haase, M.J. Lohse & S. Neubauer: Dobutamine-stress magnetic resonance microimaging in mice: acute changes of cardiac geometry and function in normal and failing murine hearts. *Circ Res* 88, 563-569 (2001)
100. Stenbit A.E., E.B. Katz, J.C. Chatham, D.L. Geenen, S.M. Factor, R.G. Weiss, T.S. Tsao, A. Malhotra, V.P. Chacko, C. Ocampo, L.A. Jelicks & M.J. Charron: Preservation of glucose metabolism in hypertrophic GLUT4-null hearts. *Am J Physiol Heart Circ Physiol* 279, H313-H318 (2000)
101. Halonen S.K., G.A. Taylor & L.M. Weiss: Gamma interferon-induced inhibition of *Toxoplasma gondii* in astrocytes is mediated by IGTP. *Infect Immun* 69, 5573-5576 (2001)
102. Uyemura S.A., S. Albuquerque & C. Curti: Energetics of heart mitochondria during acute phase of *Trypanosoma cruzi* infection in rats. *Int J Biochem Cell Biol* 27, 1183-1189 (1995)
103. Omerovic E., M. Basetti, E. Bollano, M. Bohlooly, J. Tornell, J. Isgaard, A. Hjalmarson, B. Soussi & F. Waagstein: In vivo metabolic imaging of cardiac bioenergetics in transgenic mice. *Biochem Biophys Res Commun* 271, 222-228 (2000)
104. Weiss R.G., J.C. Chatham, D. Georgakopoulos, M.J. Charron, T. Wallimann, L. Kay, B. Walzel, Y. Wang, D.A. Kass, G. Gerstenblith & V.P. Chacko: An increase in the myocardial PCr/ATP ratio in GLUT4 null mice. *FASEB J* 16, 613-615 (2002)
105. Henson R.E., S.K. Song, J.S. Pastorek, J.J. Ackerman & C.C. Lorenz: Left ventricular torsion is equal in mice and humans. *Am J Physiol Heart Circ Physiol*. 278, H1117-H1123 (2000)
106. Ross A.J., Z. Yang, S.S. Berr, W.D. Gilson, W.C. Petersen, J.N. Oshinski & B.A. French: Serial MRI evaluation of cardiac structure and function in mice after reperfused myocardial infarction. *Magn Reson Med* 47, 1158-1168 (2002)
107. Wiesmann F, A. Frydrychowicz, J. Rautenberg, R. Illinger, E. Rommel, A. Haase & S. Neubauer: Analysis of right ventricular function in healthy mice and a murine model of heart failure by in vivo MRI. *Am J Physiol Heart Circ Physiol* 283, H1065-H1071 (2002)
108. Tang B, L.A. Jelicks & D.E. Gutstein: A robust algorithm of centerline for heart image analysis. *Proc Int Soc Magn Reson Med* 10, 2464 (2002)

Key Words: Myocarditis, Echocardiography, Magnetic resonance imaging, Cardiac imaging, Chagas' disease, Cardiomyopathy, Review

Send correspondence to: Jamshid Shirani, M.D., The Jack D. Weiler Hospital of the Albert Einstein College of medicine, Division of Cardiology, 1825 Eastchester Road, Room W1-70, Bronx, NY 10461, Tel: 718-904-4009, Fax: 718-904-2075, E-mail jshirani@montefiore.org